

Failure analysis of single-bolted joint for lightweight composite laminates and metal plate

Linjie Li¹, Junli Qu¹ and Xiangdong Liu¹

¹ Department of Mechanics, Xi'an University of Science and Technology, 58 Yanta Road, Beilin District, Xi'an 710054, China
E-mail: linjie_happy@163.com

Abstract. A three-dimensional progressive damage model was developed in ANSYS to predict the damage accumulation of single bolted joint in composite laminates under in-plane tensile loading. First, we describe the formulation and algorithm of this model. Second, we calculate the failure loads of the joint in fibre reinforced epoxy laminated composite plates and compare it with the experiment results, which validates that our model can appropriately simulate the ultimate tensile strength of the joints and the whole process of failure of structure. Finally, this model is applied to study the failure process of the light-weight composite material (USN125). The study also has a great potential to provide a strong basis for bolted joints design in composite Laminates as well as a simple tool for comparing different laminate geometries and bolt arrangements.

1. Introduction

Composite is a state-of-art material in aircraft structure. To have a safer structural designs of aircraft with low weight, more and more advanced composites have been developed, which are not only light weight but also have higher strength to weight ratio [1]. One of the most useful applications of laminated composites as weight reducing elements is in aircraft wing where composite stringers has huge potential of being attached with the wing skin by means of a bolted joint [2]. Although composite materials are now being widely used as primary aircraft structures, the use is rather limited due to lack of research in composite mechanics and complicated failure mechanics of the composite joints, especially for the advanced composites [3].

2. Numerical simulations using ANSYS

2.1 The geometry of the component

The test specimen configuration is shown in Figure 1, and the specific values are shown in Table 1.

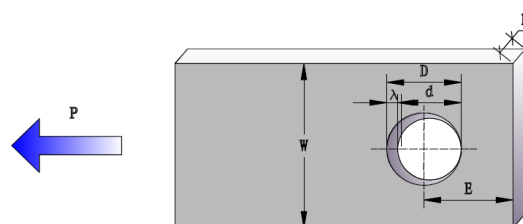


Figure 1. Geometries of the specimens

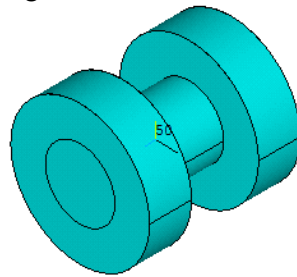
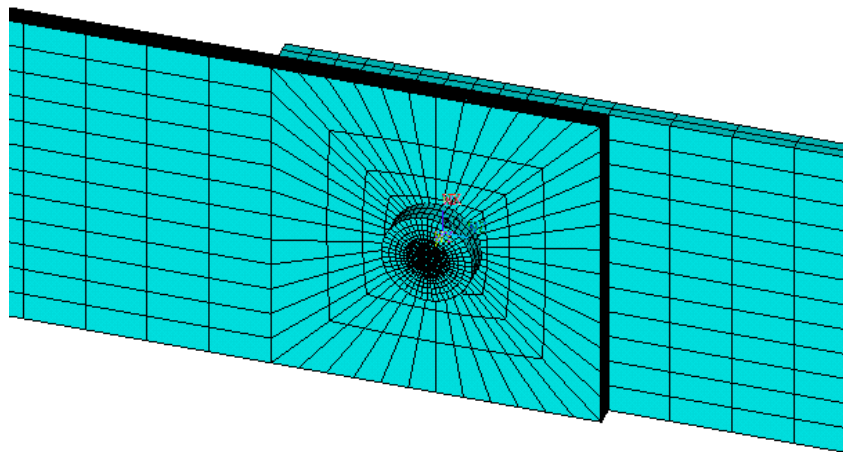
Table 1. Geometrical model of the composite joint.

| Plate length (mm) | Plate thickness (mm) | Hole diameter (mm) | Plate width (mm) | Distance between the center of the hole and the right margin of plate(mm) |
|----------------------|-------------------------|-----------------------|---------------------|--|
| 160.00 | 2.00 | 4.14 | 30.00 | 15.00 |

2.2 Finite element modeling

As shown in Figure 2, bolts, nuts and gaskets are simplified as a whole in this 3D model. The metal plate and bolt are modelled using Solid185 elements and the composite plate is modelled using Shell99 in ansys software. In order to make the simulation closer to the real situation, the impact of the contact model, frictional and preload were also considerate. The contact areas between bolt and plates are modelled using CONTA173 contact element. The magnitude of the frictional force between the contact surfaces is controlled by coulomb friction, the friction coefficient was 0.2. The preload applied on the bolt is 3 N·m.

The boundary conditions are shown in the Figure 3. The right edge of the model is fixed ($U_x = U_y = U_z = \phi_x = \phi_y = \phi_z = 0$) and a uniformly increasing tensile-load is applied on the left edge of the composite plate along the x-axial direction of the model ($U_y = U_z = \phi_x = \phi_y = \phi_z = 0$). The mesh convergence analysis is performed on a various number of elements to ensure the accuracy of calculations and freedom of the model to mesh size. The final mesh distributions through thickness and around the bolt hole are shown in Figure 3.

**Figure 2.** Simplified model of bolt**Figure 3.** FEM mesh of composite joint

3. Analysis of failure

3.1 Laminated plate cumulative damage analysis processing

Dano et al. [4] developed a progressive damage model to investigate the effect of failure criteria and the material property degradation rules on the behaviour of joints in a graphite/epoxy composite laminate. A flow chart for the program is shown in Figure 4.

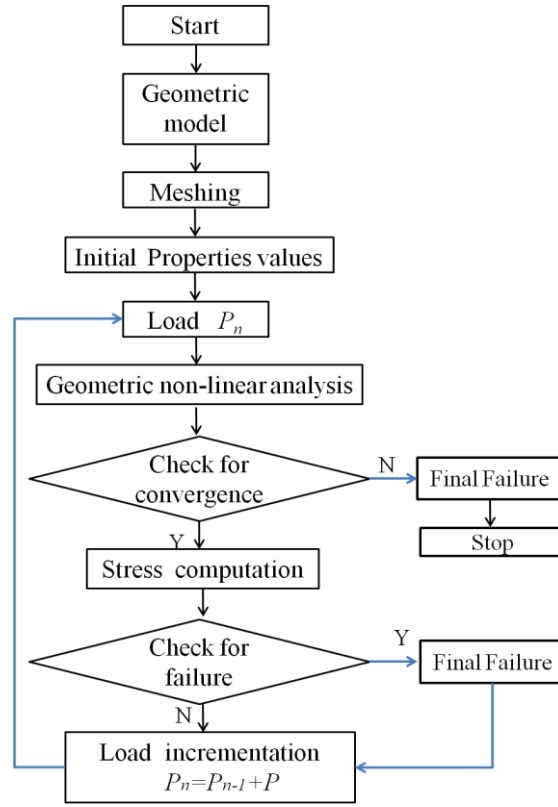


Figure 4. Progressive damage model algorithm

3.2 Stress analysis

Apply a constraint to one end of the composite laminates and apply load to another end. The load acting on the inner surface of the laminate increases gradually, when the load increases to a step n , i.e. $P_n = P_{n-1} + P$. Because there is no volume force and according to incremental form of virtual displacement principle and force boundary conditions, we have balance equation as follows.

$$\int_{V_{n-1}} \sigma_{ij}^n \delta(\Delta \varepsilon_{ij}) dV - \int_{S_\sigma} \bar{T}_i^n \delta(\Delta u_i) dS = 0 \quad i, j = 1, 2, 3, \quad (1)$$

where $\Delta \varepsilon_{ij}$ and Δu_i represent strain increment and displacement increment from the load step $n-1$ to the load step n , respectively. σ_{ij}^n represent the laminates stress under load P_n , $\sigma_{ij}^n = \sigma_{ij}^{n-1} + \Delta \sigma_{ij}$, where $\Delta \sigma_{ij}$ is the incremental load from load step $n-1$ to the load step n . \bar{T}_i^n represent the per unit area force acting on the boundary S_σ under load P_n . V_{n-1} is the volume deformation at step $n-1$. Due to the geometric large deformation, strain increment is shown below.

$$\Delta \varepsilon_{ij} = \Delta e_{ij} + \Delta \eta_{ij}, \quad (2)$$

where Δe_{ij} is the strain increment and $\Delta \eta_{ij}$ is the quadratic term. The stress-strain relationship of anisotropic elastomers is shown below [5].

$$\sigma_i = \sum_{j=1}^6 C_{ij} \varepsilon_j \quad (i = 1, 2, \dots, 6). \quad (3)$$

When the load from the step $n-1$ to step n , the increased load variable is $\Delta\sigma_i = C_{ijkl}^{n-1} \Delta\epsilon_{kl}$, where C_{ijkl}^{n-1} is the composite material modulus under the load step $n-1$, which can be obtained by the following equation.

$$C_{ijkl}^{n-1} = C_{rs}^{n-1} = \sum_{k=1}^m \left[\frac{\overline{Q}_{rs}^{(k)}}{m} \right]^{n-1}, \quad (4)$$

where m is the number of composite layers. $\left[\overline{Q}_{rs}^{(k)} \right]^{n-1}$ is the composite material modulus of the k -th layer after converted by coordinates under the $n-1$ load step. $\Delta\epsilon_{ij}$ and $\Delta\sigma_{ij}$ are liberalized: $\Delta\epsilon_{ij} = \Delta e_{ij}$, $\Delta\sigma_i = C_{ijkl}^{n-1} \Delta e_{kl}$, then the equation (1) can be converted into equation (5):

$$\int_{n-1} C_{ijkl}^{n-1} \Delta e_{kl} \delta(\Delta e_{ij}) dV + \int_{n-1} \sigma_{ij}^{n-1} \delta(\Delta \eta_{ij}) dV = \int_{s_\sigma} \overline{T}_i^n \delta(\Delta u_i) dS - \int_{n-1} \sigma_{ij}^n \delta(\Delta e_{ij}) dV. \quad (5)$$

The result of the variation equation on the above equation will give a linear system of equations for displacement increments, which can be further solved by finite element method. When the load increases to P_n , if the material damage occurs, it will lead to damage to the material properties of the damage zone, that is, the material modulus part of the damage area will change, the specific degradation will be described in the lower part. With the advent of damage, structural stress and strain will reassign, the equation (5) is calculated. The process is repeated until there is no new damage occurs.

3.3 Material degradation rule

With the increasing of load, the fibre and matrix of the laminated plate are gradually destroyed. The structural rigidity is decreasing, and the expansion of the damage can be characterized by the degradation of the elastic constants of the material. Tan [6] used parameters degradation to analysis the cumulative damage process as shown in Table2.

Table 2. Material degradation of Tan's rule

| Failure Mode | Tan's rule |
|-----------------------------|--|
| Matrix tensile cracking | $E_{22} \rightarrow 0.2E_{22}, G_{12} \rightarrow 0.2G_{12}, G_{23} \rightarrow 0.2G_{23}$ |
| Matrix compressive cracking | $E_{22} \rightarrow 0.4E_{22}, G_{12} \rightarrow 0.4G_{12}, G_{23} \rightarrow 0.4G_{23}$ |
| Fiber tensile cracking | $E_{11} \rightarrow 0.07E_{11}$ |
| Fiber compressive cracking | $E_{11} \rightarrow 0.07E_{11}$ |
| Fiber-matrix shear out | $G_{12} = \nu_{12} = 0$ |
| Delamination in tension | $E_{33} = G_{23} = G_{13} = \nu_{23} = \nu_{13} = 0$ |
| Delamination in compression | $E_{33} = G_{23} = G_{13} = \nu_{23} = \nu_{13} = 0$ |

3.4 Hashin's failure criteria [7]

Hashin's failure Criteria is popular in the composite industry due to its elegant form and accuracy matching the experimental results. The three-dimensional Hashin guideline expression is shown below:

(1) Fiber tensile cracking ($\sigma_{11} > 0$)

$$F_f^2 = \left(\frac{\sigma_{11}^2}{X_t} \right) + \left(\frac{\tau_{12}}{S_{12}} \right)^2 + \left(\frac{\tau_{13}}{S_{13}} \right)^2 \geq 1 \quad (6)$$

(2) Fiber compressive cracking ($\sigma_{11} > 0$)

$$F_f^2 = \left(\frac{\sigma_{11}^2}{X_c^2} \right) \geq 1. \quad (7)$$

(3) Matrix tensile cracking ($\sigma_{22} + \sigma_{33} \geq 0$)

$$F_m^2 = \left(\frac{\sigma_{22} + \sigma_{33}}{Y_t} \right)^2 + \frac{(\tau_{23} - \sigma_{22}\sigma_{33})^2}{S_{23}^2} + \left(\frac{\tau_{12}}{S_{12}} \right)^2 + \left(\frac{\tau_{13}}{S_{13}} \right)^2 \geq 1. \quad (8)$$

(4) Matrix compressive cracking ($\sigma_{22} + \sigma_{33} < 0$)

$$F_m^2 = \frac{1}{Y_c} \left(\left(\frac{Y_c}{2S_{12}} \right)^2 - 1 \right)^2 (\sigma_{22} + \sigma_{33}) + \left(\frac{\sigma_{22} + \sigma_{33}}{2S_{12}^2} \right)^2 + \frac{(\tau_{23}^2 - \sigma_{22}\sigma_{33})}{S_{23}^2} + \left(\frac{\tau_{12}}{S_{12}} \right)^2 + \left(\frac{\tau_{13}}{S_{13}} \right)^2 \geq 1. \quad (9)$$

(5) Fiber-matrix shear out ($\sigma_{11} > 0$)

$$F_m^2 = \left(\frac{\sigma_{33}}{Y_c} \right)^2 + \left(\frac{\tau_{12}}{S_{12}} \right)^2 + \left(\frac{\tau_{13}}{S_{13}} \right)^2 \geq 1, \quad (10)$$

where σ_{ii} ($i=1,2,3$) represent the normal stress in the i direction and τ_{ij} ($i, j=1,2,3$) is the shear stress in the i, j plane. X_t, X_c, Y_t, Y_c represent the tensile strength and compressive strength of the fibre direction and in the plane perpendicular to the fibre direction, respectively. S_{ij} ($i, j=1,2,3$) represent the shear strength in-plane. F_j ($j=f, m$) is the failure factor which can be used to characterize the degree of the material damage. The greater the failure factor is, the more serious the damage is. When the failure factor is greater than 1, the material will be failure.

4. Validation of the numerical simulations

In order to verify the accuracy of the model, specimens with the same size and material (CCF300/QY8911) as that used in Ref 8 are calculated and analysed. The mechanical properties of the composite are shown in Table 3. The stacking sequences for the composite ply is [45/0/-45/90/45/0/-45/0]_s and the thickness of each ply is 0.125mm.

Table 3. Material properties of composite material (CCF300/QY8911).

| Material properties | E_{11} (GPa) | E_{22} (GPa) | E_{33} (GPa) | G_{12} (GPa) | G_{23} (GPa) | X_t (MPa) | G_{13} (GPa) | | |
|---------------------|----------------|----------------|----------------|----------------|----------------|-------------|----------------|------------|--|
| CCF300/QY8911 | 133 | 9.9 | 9.9 | 6.67 | 6.67 | 2134.2 | 3.9 | | |
| | | | | | | | | | |
| X_c (MPa) | Y_t (MPa) | Y_c (MPa) | S_{12} (MPa) | S_{13} (MPa) | S_{23} (MPa) | ν_{12} | ν_{13} | ν_{23} | |
| 1121.2 | 33.0 | 191.3 | 87 | 87 | 110 | 0.27 | 0.27 | 0.27 | |

In Table 3, E_{11} , E_{22} and E_{33} mean the elastic modulus in longitudinal direction and transverse direction, respectively. G_{12} , G_{13} and G_{23} are the in plane and the out-of plane shear modulus, respectively. X and Y are the strength in direction of warp and fil, respectively. S is shear strength. Subscript t and c mean the tensile and compressive properties. ν is Poisson's ratio.

The material properties of metal plate and bolt are $E_t = 115$ GPa, $\nu = 0.31$ and $S = 675$ MPa, where S represents the shear strength. The configuration of single-lap bolt joint was shown in Figure 5.

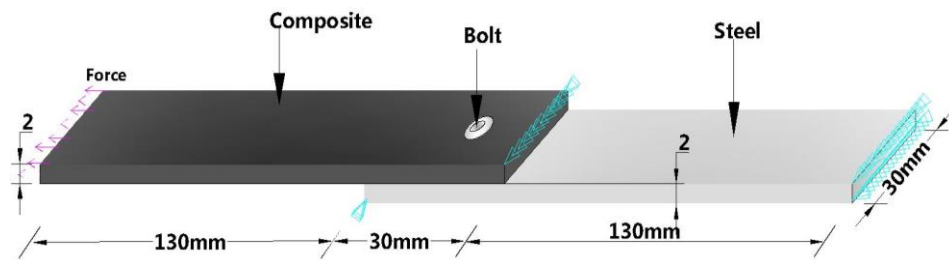


Figure 5. Configuration of single-lap bolted joint

Figure 6 and Table 4 show the comparison between the results of the simulation and experimental results under static tensile loading, respectively.

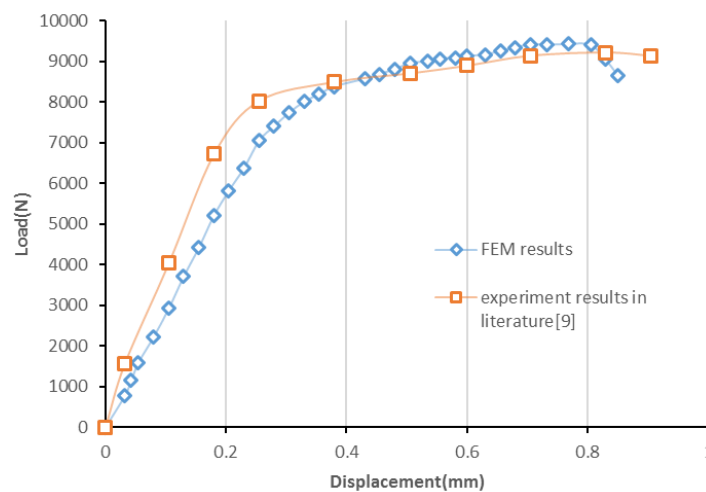


Figure 6. Comparison of FEM simulation result and experiment result

Table 4. Comparison of testing and numerical results

| Items | Numerical result | Test result [8] | Relative Errors/% |
|--------------------------------|------------------|-----------------|-------------------|
| Failure load(kN) | 9.414 | 9.2 | 2.32 |
| Stiffness(N mm ⁻¹) | 142.195 | 137.8 | 3.19 |

According to the comparison presented above, the error between simulated prediction value and experimental results is less than 5%, indicating that this model can successfully be applied to predict the strength of advance composites, as well as to comparison of different joint configurations and effect of design parameters.

5. Failure analysis for lightweight composite laminates

Use our model to simulate the damage process and failure of light-weight composite (USN125) laminates. The material properties are listed in Table.5 and the ply is [45/0/-45/90/45/0/-45/0]_s.

Table 5. Material properties of composite material (USN125). [9]

| Material Properties | E_{11} (GPa) | E_{22} (GPa) | E_{33} (GPa) | G_{12} (GPa) | G_{23} (GPa) | G_{13} (GPa) | X_t (MPa) |
|---------------------|----------------|----------------|----------------|----------------|----------------|----------------|-------------|
| USN125 | 162 | 9.6 | 9.6 | 6.1 | 3.5 | 6.1 | 2552 |

| X_c (MPa) | Y_t (MPa) | Y_c (MPa) | S_{12} (MPa) | S_{13} (MPa) | S_{23} (MPa) | ν_{12} | ν_{13} | ν_{23} |
|-------------|-------------|-------------|----------------|----------------|----------------|------------|------------|------------|
| 2552 | 43 | 43 | 94 | 94 | 40 | 0.298 | 0.298 | 0.470 |

Figure 7 illustrates the initial stress states of the composite laminate. It can be seen from the stress component contour diagram that the lattice around the bolt hole of the composite material changes more obviously, especially in the direction of -45° , which indicates that the fiber orientation of the -45° layer would firstly reach the maximum bearing strength. In high compression zone, due to high values of S33, i.e. of principle stress along laminate thickness, there exists a strong potential of delamination due to compression, thus causing a typical bearing failure. It has also been observed that shearing stress in yz-plane (S23) and xz-plane (S13) are very low as compared to shearing stress in xy-plane (S12) and the transverse compressive stress of the fiber is lower than the shearing stress.

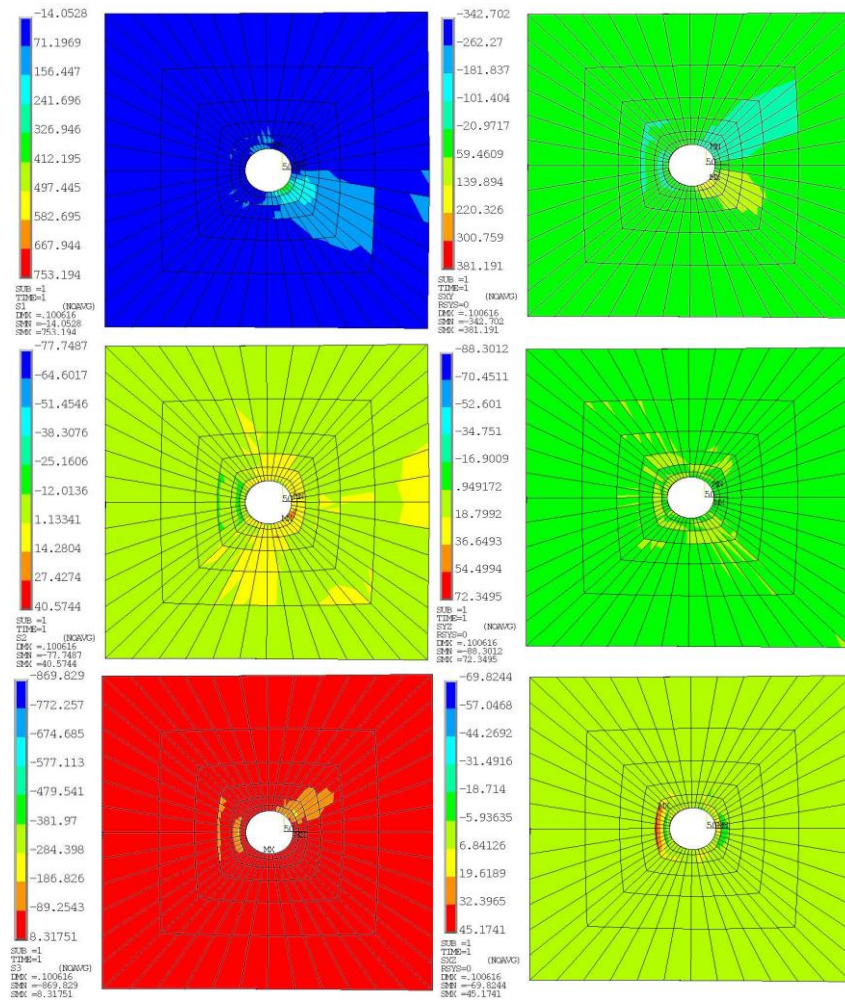


Figure 7. Stress component cloud state variables results

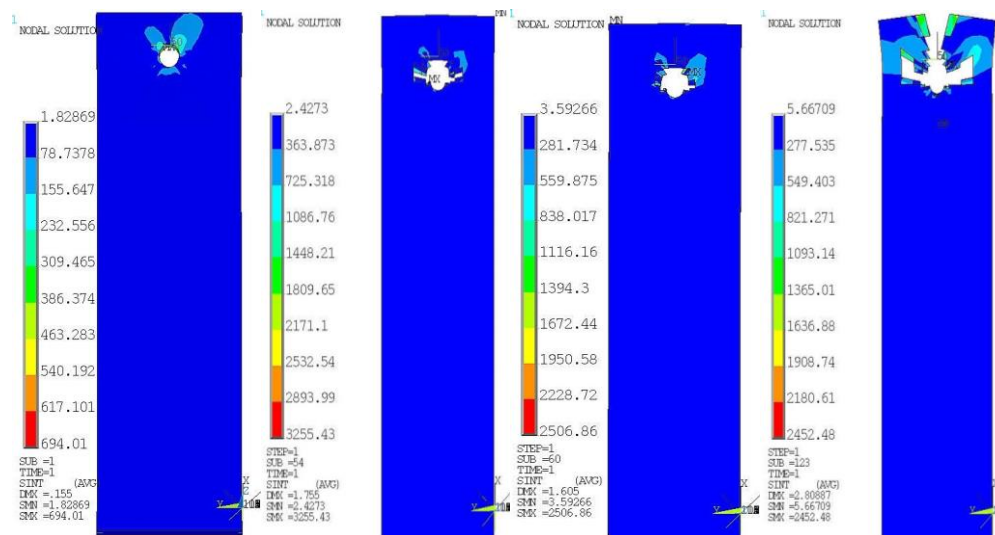


Figure 8. Stress distribution of bolt-hole and progressive damage of laminate

From Figure 8, we visualize the stress and deformation progressively. It is observed that most of the applied load is contributed towards compression along fiber directions. Remarkable tensile stress transverse to the direction of laminate is near the hole which may cause the effect of matrix cracking. However, because the region under compressive load is reasonably more as compared to region in tensile stress, there are more chances of bearing failure of the joint. The inter lamina stresses of both 90° plies with their neighboring plies may cause delamination, thus to effect the ultimate failure load. There is a warp between the composite laminates and the metal plates during the stretching process, and there is a tendency to be separated, and the bolt is inclined in the stretching direction.

6. Conclusions

In this study, a three-dimensional Progressive Damage Model was developed to compute the tensile strength and the maximum load of the composite metal joint damage accumulation failure analysis model, considering the preload, friction and complex contact area of connection and contact deformation. According to the study, conclusions are as follows.

(1) The tensile strength and the maximum load of the composite (CCF300/QY8911)-metal joint are 142.195MPa and 9.414kN, respectively. The results of the experimentation are 124.5MPa and 9.2kN. The error between simulation and experiment result is less than 5%, indicating that this model can be applied to predict the strength of advance composites.

(2) The failure process and failure load of the lightweight composite (USN125)-metal joint were obtained by the established model. The initial failure crack occurs in the direction of -45° and 45° of the fiber layer and the matrix separation of the stress generated in the direction of -45° , so that the direction of -45° fiber bear the main load.

(3) Since the error is very stable between simulated strength prediction value and experimental value of strength so the model in the paper can successfully be applied for comparison of different joint configurations and effect of design parameters for single bolted joint but it's necessary to validate the three-dimensional finite model and calculation method in this paper in multiple-bolted joints in further study.

7. References

- [1] Starikov R, Schon J. Quasi-static Behaviour of Composite Joints with Protruding Head Bolts. *Compos Struct* 2001; 51:411-25.
- [2] Saqib Mehmood, Zhao Libin and Huang Hai. Failure Analysis of Single and Double Bolted Joints for Composite Laminates. *12th International Bhurban Conference on Applied Sciences & Technology* 2011;15: 49-54.

- [3] Thoppul S D, Finegan J, Gibson. Mechanics of Mechanically Fastened Joints in Polymer-matrix Composite Structures -a review. *Compos Sci Techno* 2009; 69: 301-29.
- [4] Dano ML, Kamal E, Gendron G. Analysis of Bolted Joints in Composite Laminates: strains and bearing stiffness predictions. *Compos Struct* 2007; 79(4):562-70.
- [5] Shen GL, Hu GK. *Mechanics of Composite Materials*[M]. Tsing Hua University Press 2006.
- [6] Tan SC, Perez J. Progressive Failure of Laminated Composites with a Hole under Compressive Loading. *J Reinf Plas Compos* 1993; 12:1043-1057.
- [7] Hashin Z. Failure Criteria for Unidirectional Fibre Composites. *Applied Mechanics* 1980; 47(2): 329-334.
- [8] Liu X K, Zhang WW, Li Y Z. Investigation on the Deformation Failure of Single-bolted Metal to Composite Joints. *Science Technology and Engineering* 2014; 22(14):307-311.
- [9] Seong MS, Kim TW, Nguyen KH, Kweon JH and Choi JH. A Parametric Study on the Failure of Bonded Single Lap Joints of Carbon Composite and Aluminium. *Compos Struct* 2008; 86:135-145.